

RSC Advances



This is an *Accepted Manuscript*, which has been through the Royal Society of Chemistry peer review process and has been accepted for publication.

Accepted Manuscripts are published online shortly after acceptance, before technical editing, formatting and proof reading. Using this free service, authors can make their results available to the community, in citable form, before we publish the edited article. This *Accepted Manuscript* will be replaced by the edited, formatted and paginated article as soon as this is available.

You can find more information about *Accepted Manuscripts* in the [Information for Authors](#).

Please note that technical editing may introduce minor changes to the text and/or graphics, which may alter content. The journal's standard [Terms & Conditions](#) and the [Ethical guidelines](#) still apply. In no event shall the Royal Society of Chemistry be held responsible for any errors or omissions in this *Accepted Manuscript* or any consequences arising from the use of any information it contains.



Journal Name

ARTICLE

Highly efficient colorimetric detection of cancer cells utilizing Fe-MIL-101 with intrinsic peroxidase-like catalytic activity over broad pH range

Received 00th January 20xx,
Accepted 00th January 20xx

DOI: 10.1039/x0xx00000x

www.rsc.org/

Daomei Chen, Bin Li,* Liang Jiang, Deliang Duan, Yizhou Li, Jiaqiang Wang,* Jiao He and Yanbo Zeng

Early diagnosis and timely treatment of cancer are the keys to improve patient survival rate at present. Metal-organic frameworks (MOFs) consisting of infinite crystalline lattices with metal clusters and organic linkers may provide opportunities for detection cancer cells which has remained unknown. Herein, we report that Fe-MIL-101 possesses an intrinsic enzyme mimicking activity similar to that found in natural horseradish peroxidase and shows highly catalytic activity even at neutral pH. The Michaelis constant (K_m) of Fe-MIL-101 with H_2O_2 as the substrate is about 616-fold (at pH 4.0) and 20-fold (at pH 7.0) smaller than free natural horseradish peroxidase (HRP), indicating a much higher affinity for H_2O_2 than HRP and most of the peroxidase mimetics. Moreover, Fe-MIL-101 was successfully used to detect cancer cells by conjugating folic acid onto Fe-MIL-101 without any surface modification. The detection limit of the method for Hela was estimated to be 50 cells and the reaction colour produced by 10 cells also could be observed by the naked eye. The proposed method holds considerable potential for simple, sensitive, universal, and specific cancer cell detection.

Introduction

Clinical diagnostics, toxicity monitoring, and public health protection require early and accurate detection of carcinoma cells in blood or tissue. A number of systems including polymerase chain reaction (PCR)-based methods, cytometry, colorimetric assay, fluorescence, surface plasmon resonance and microfluidics have been reported.¹⁻⁵ However, a majority of these methods are expensive, time-consuming, need complex fluorescence labeling or require expensive instrumentation, and are not adequate for point-of-care applications.⁵⁻⁷ Due to the increasing demand of control of various diseases, the development of more sensitive, less expensive, and rapid detection method for early diagnosis of cancer has been of great importance. To this end, a number of biosensors based on enzyme-mimetic inorganic materials have been developed to serve as a new class of ideal and important colorimetric detection tools for biosensing, owing to their high stability, easy preparation, controllable structure and composition, and tunable catalytic activity.^{8,9} So far, a great

quantity of inorganic nanoparticles, especially those formed from noble metals, such as lysozyme stabilized gold nanoclusters and graphene oxide (GO-AuNCs) hybrid,¹⁰ porous platinum nanoparticles on graphene oxide (PtNPs/GO) nanohybrid,¹¹ chitosan modified silver halide (AgX, X = Cl, Br, I) (CS-AgX) nanoparticles,¹² graphene oxide-magnetic-platinum (GO_MNP-Pt) nanohybrids¹³ and nanoparticle-loaded mesoporous silica-coated graphene (GSF@AuNPs) nanohybrid¹⁴ have been found to possess intrinsic peroxidase-like activity. In comparison with natural horseradish peroxidase (HRP), these nanoparticles were more stable against denaturation or protease digestion and their preparation and storage were relatively simple. These enzyme-like nanomaterials could be used in a variety of applications, such as detection of immunoassay, glucose and so on. Recently, nanomaterials have been conjugated folic acid through sulfonation or amidation, such as PtNPs/GO,¹¹ CS-AgX,¹² GO-AuNCs¹⁰ and GSF@AuNPs¹⁴ for detecting cancer cells, which was based on folic acid can specifically target folate receptors overexpressed on the surface of different types of cancer cells.^{15,16} The detection limit of the PtNPs/GO for MCF-7 was estimated to be as low as 30 cells, which was the lowest among those reported by the method using peroxidase mimetics based on nanomaterials. However, the immunoassay of the materials without any surface modification was seldom explored.

On the other hand, metal-organic frameworks (MOFs), formed by association of metal centers or clusters and organic

Yunnan Province Engineering Research Center of Photocatalytic Treatment of Industrial Wastewater, The Universities' Center for Photocatalytic Treatment of Pollutants in Yunnan Province, Key Laboratory of Medicinal Chemistry for Natural Resource, Ministry of Education, School of Chemical Sciences & Technology, Yunnan University, Kunming 650091, P.R. China. E-mail: libin36@ynu.edu.cn (B. Li); jqwang@ynu.edu.cn (J. Wang). Fax: (+)86 871 65031567.

*Electronic Supplementary Information (ESI) available: [details of any supplementary information available should be included here]. See DOI: 10.1039/x0xx00000x

linkers, is gaining importance in materials science and biotechnology because of its outstanding properties, including an unprecedentedly large and permanent inner porosity.¹⁷⁻²³ Interestingly, MOF PCN-222(Fe) with porphyrinic Fe(III) centers,²⁴ Fe(III)-based MIL-53,²⁵ HKUST-1,²⁶ Fe-MIL-88NH₂,^{27,28} MIL-68 (Fe) and MIL-100(Fe)²⁹ were very recently reported to show intrinsic peroxidase-like catalytic activity for detection H₂O₂, glucose and ascorbic acid. As a new attempt, we found that Cu-MOF (or MOF-199, HKUST-1) possesses an intrinsic enzyme mimicking activity similar to that found in natural trypsin to bovine serum albumin (BSA) and casein.³⁰ These findings and previous peroxidase mimics findings induce us to call them "MOFzymes" in analogy to the nomenclature of "nanozymes".^{31,32}

Although these limited examples demonstrate the potential of MOFs to replace HRP in various biosensing applications, the detection of cancer cells using MOFs has not been exploited so far as we know. Furthermore, the optimum reaction usually occurred in acidic solution with a pH near 4 for these MOFs enzyme mimics, which greatly limits its applications in biological systems where a near neutral pH is required. So far as we know, there is no report on using nanomaterials except for AuNCs,¹⁰ CS-AgX¹² and GO_MNP-Pt¹³ let alone MOFs for peroxidase mimetics with high catalytic activity over a broad pH range, in particular at neutral pH. Therefore, there is a strong need to develop enzyme mimics that are able to exhibit high catalytic activity over a broad pH range, especially near neutral pH values.

Herein, in the continuation of our work, we take advantage of the folic acid conjugated Fe-MIL-101 without any surface modification to design and develop a simple, cheap, highly selective and sensitive colorimetric assay to detect cancer cells based on its intrinsic peroxidase-like activity. The detection limit of the method for HeLa was estimated to be as low as 50 cells, and the reaction colour produced by 10 cells also could be observed by the naked eye which was the lowest among the methods using peroxidase mimetics based on nanomaterials as we know. It aims to provide new insights into the application of MOFs in biosensing.

Experimental

Chemicals and instrumentation.

All chemicals were of analytical grade and used without further purification. Terephthalic acid (H₂BDC, 99%), ferric chloride hexahydrate (FeCl₃•6H₂O, 99%), ethanol (99.5%), and N, N -dimethylformamide (DMF, 99.9%) were purchased from Sinopharm Chemical Reagent Co. (Beijing, China) and used for synthesis. Folic acid (FA), 3, 3', 5, 5'-tetramethylbenzidine (TMB) and 2, 2'-azino-bis (3-ethylbenzothiazoline-6-sulfonic acid) diammonium salt (ABTS) were obtained from BBI (Ontario, Canada). Dimethyl sulfoxide (DMSO) and MES buffer were purchased from Feng Chuan Chemicals Reagent Co. Ltd (Tianjin, China). Penicillin and streptomycin were purchased

from Sigma Chemical Co. Ltd., (St. Louis, MO, USA). DMEM medium and fetal bovine serum was purchased from Hyclone Laboratories (Logan, UT).

Pore size distributions, BET surface areas and pore volumes were measured by nitrogen adsorption/desorption measurements using a micromeritics tristar II surface area and porosity analyzer. Prior to the analysis, the samples were degassed at 90°C for 1h. X-ray powder diffraction (XRD) experiments were conducted on a D/max-3B spectrometer with Cu K α radiation. Scans were made in the 2 θ range 3-80° with a scan rate of 10° min⁻¹ (wide angle diffraction). Fourier transform infrared (FT-IR) measurements were performed on a Nicolet 8700 Instrument. Inductively coupled plasma-atomic emission spectrometry (ICP-AES) analysis was used to determine the contents of Fe³⁺ released from Fe-MIL-101. ICP-AES measurement was carried out with a Shimadzu ICPS-1000IV model. The ICP-MS detection was achieved using a model 7700 ICP-MS (Agilent). A Shimadzu UV-2450 spectrophotometer and Spectra max 190 microplate spectrophotometer were used to measure absorbance. Fluorometric measurement was carried out by F-7000FL Spectrophotometer. Scanning electron microscopy (SEM) images of the samples were taken on a FEI Quanta 200FEG microscope. The determinations of zeta potential and size of the nanoparticles were carried out using Zetasizer Nano-ZS (Malvern Instruments Ltd, UK). Each data point for zeta potential is an average of at least 5 measurements at pH 7.0 (in PBS and in DMEM cell culture medium + 10% fetal bovine serum).

Syntheses of materials.

Metal-organic framework Fe-MIL-101 was prepared by a mild solvothermal process based on reported works.³³ FeCl₃•6H₂O and H₂BDC were added slowly into DMF solution. The mixture was stirred for 10 min at room temperature, and then transferred into a Teflon-lined stainless steel autoclave and heated at 110 °C for 20 h. The resulting brown solid was filtered off, and the raw product was purified by washing in hot ethanol (70 °C, 3 h), filtered off, and dried in an oven (70 °C, 30 min). The particles were isolated by centrifuging and washed with DMF and ethanol to remove any unreacted starting materials.

To conjugate Fe-MIL-101 with folic acid (FA), free folic acid (10 mg, 0.0227 mmol) was dissolved in 4 mL 50 mM MES buffer (pH 6.0). After agitating overnight at temperature in the dark, the solution of Fe-MIL-101-FA (20 mg) was added to the mixture. The resulting solution was stirred at room temperature for 24 h and then centrifuged at 13000 rpm to separate the precipitate. The precipitate was washed three times with ultrapure water to remove the unreacted folic acid.

Evaluation of peroxidase-like activity of Fe-MIL-101.

The effect of pH, temperature, H₂O₂ concentration and TMB concentration on the peroxidase-like activity of Fe-MIL-101 was carried out in a reaction volume of 5 mL sodium acetate

and acetate buffer (20 mM). The steady state kinetic assays of Fe-MIL-101 were investigated by varying concentrations of TMB at a fixed concentration of H₂O₂ or varying concentrations of H₂O₂ at a fixed concentration of TMB at room temperature. A typical experiment was carried out using 20 µg mL⁻¹ Fe-MIL-101 in acetate buffer solution (20 mM, pH 4.0) and borate buffer (20 mM, pH 7.0) with the presence of 0.2 mM H₂O₂ and 0.2 mM TMB as the substrate. The blue color was monitored after reaction 400 s at 652 nm using a Shimadzu UV-2450 spectrophotometer. The kinetic parameters were calculated based on the equation $v = V_{\max}([S] / (K_m + [S]))$, where v is the initial velocity, V_{\max} is the maximal velocity, $[S]$ is the concentration of the substrate, and K_m is the Michaelis constant. main text of the article should appear here with headings as appropriate.

Cell viability measurements.

All cell lines including mouse embryonic fibroblasts cells (BABL-3T3), human cervical carcinoma cells (Hela), colon adenocarcinoma cells (HT-29) and human mouth epidermal carcinoma cells (KB) were purchased from the American Type Culture Collection (ATCC, Manassas, VA, USA). The cell viability tests were performed by the standard MTT (3-(4, 5-dimethylthiazol-2-yl)-2, 5-diphenyltetrazolium bromide) assay method. Four cancer cell lines KB, HT-29, Hela and BABL-3T3 cells were plated in 96-well plates at a density of 1×10^4 cells per well. After 24 hours of culture in the normal growth medium, cells were exposed to 20 µg mL⁻¹ of Fe-MIL-101-FA, 0.2mM H₂O₂, 0.2mM TMB, 0.2mM H₂O₂+0.2mM TMB and 0.2mM H₂O₂+0.2mM TMB+ 20 µg mL⁻¹ Fe-MIL-101-FA for 12 h. Then cells were incubated with 5 µg mL⁻¹ MTT for 4 h, 150 µL DMSO was added into plates for dissolving crystals. Absorbance at 490 nm was determined by using spectra max 190 microplate spectrophotometer (Molecular Devices Corporation, USA). The experiment was repeated at least 3 times. The relative cell viability (%) of the hybrid was calculated by $[\text{OD}]_{\text{test}} / [\text{OD}]_{\text{control}}$, where $[\text{OD}]_{\text{control}}$ and $[\text{OD}]_{\text{test}}$ are the average absorbance of the control and test samples, respectively.

Colorimetric detection for cancer cells.

All cell lines including mouse embryonic fibroblasts cells (BABL-3T3), colon adenocarcinoma cell (HT-29), human cervical cancer cells (Hela) and human mouth epidermal carcinoma cells (KB) were purchased from the American Type Culture Collection (ATCC, Manassas, VA, USA). The BABL-3T3 cells line was cultured in DMEM (high glucose) and other cells were grown in DMEM (low glucose) containing 10 % fetal bovine serum and 1 % penicillin/streptomycin in a humidified atmosphere of 5 % CO₂ and 95 % air at 37 °C. In a typical test, cells were incubated with 20 µg mL⁻¹ Fe-MIL-101-FA for 1.5 h. Afterward, cells were washed by phosphate buffer three times and dispersed into 500 µL buffer solution (0.9% NaCl, pH 7.0), then 1.25 µLTMB (final concentration 0.2 mM) and 2.26 µL 0.3% H₂O₂ (final concentration 0.2 mM) were added. The absorbance of the oxidation product was monitored at 652nm

with a microplate reader (Spectra max 190 microplate spectrophotometer).

Results and discussion

The characterization of Fe-MIL-101 and Fe-MIL-101-FA.

The X-ray diffraction (XRD) pattern of the as-synthesized Fe-MIL-101 is shown in Fig. S1. The diffraction peaks are all corresponded to the products synthesized by literature³³ and the overall is agreement with a pattern calculated from crystallographic data in this reference. The adsorption-desorption isotherms of Fe-MIL-101 (Fig. S2) is of type I indicating the presence of the microporous network, which possesses a specific pore volume of 1.96 cm³ g⁻¹ and an average pore size of 2.11 nm. The Langmuir and Brunauer-Emmer-Teller (BET) surface area were 5400 m² g⁻¹ and 3710 m²g⁻¹, respectively. SEM images show that Fe-MIL-101 has a typical octahedron morphology and an average diameter of ~ 1.4 µm (Fig. S3). All the results mentioned above confirmed that Fe-MIL-101 was properly synthesized.

Fe-MIL-101-FA obtained by adsorption folic acid onto Fe-MIL-101 was confirmed by FT-IR measurements (Fig. S4). Based on the assignment of the FT-IR spectra of folic acid reported in the literature,³⁴ the FT-IR spectrum for pure folic acid was characterized by a number of characteristic bands occurring at 3400, 2920, 1693, 1607, 1482 and 1410 cm⁻¹. The bands between 3500 and 3000 cm⁻¹ are due to the hydroxyl (OH) stretching and NH- stretching vibration bands. The C=O bond stretching vibration of carboxyl group appears at 1693cm⁻¹. The band at 1607cm⁻¹ relates to the bending mode of NH- vibration and at 1410cm⁻¹ corresponds to OH deformation band of phenyl skeleton. The band at 1482 cm⁻¹ was attributed to characteristic absorption band of the phenyl ring. As shown in FT-IR of Fe-MIL-101-FA, three new peaks at 2920,1693, 1482cm⁻¹ appeared after adsorption of FA, which correspond to C=O bond stretching vibration of carboxyl group, -C-H symmetric and asymmetric stretching vibration and absorption band of the phenyl ring, respectively. The higher intensity of the characteristic absorption bands at 1607 cm⁻¹ and 1410 cm⁻¹ were observed after reaction with FA, which correspond to FA linked onto the surface of Fe-MIL-101. Moreover, the amount of folic acid conjugated on Fe-MIL-101 was determined by quantitative ultraviolet (UV) spectrophotometric analysis and evaluated by measuring the absorbance of the product at 358 nm (folic acid $\epsilon=15,760 \text{ M}^{-1} \text{ cm}^{-1}$). It was found that about $8 \pm 1.2\%$ FA was adsorbed on Fe-MIL-101. To further verify the presence of folic acid on Fe-MIL-101, the size of Fe-MIL-101 and Fe-MIL-101-FA was detected by Zetasizer Nano-ZS. Table S1 shows that the size of Fe-MIL-101 changed from $1368 \pm 70 \text{ nm}$ to $1620 \pm 18 \text{ nm}$ after adsorption FA. These observations implied FA was successfully adsorbed on the surface of Fe-MIL-101.

Peroxidase-like activity of Fe-MIL-101.

The peroxidase-like activity of Fe-MIL-101 was evaluated by the traditional catalytic oxidation of peroxidase substrate TMB

in the presence of H_2O_2 . As shown in Fig. 1, in the absence and presence of H_2O_2 , a colorless TMB solution was observed, which displayed a negligible absorption at maximum absorbance 652 nm, indicating that no oxidation reaction occurred in the absence of Fe-MIL-101. In contrast, Fe-MIL-101 could catalyze the oxidation of TMB in the presence of H_2O_2 (Fig. 1A) and produce a deep blue color, with a maximum absorbance at 652 nm, indicating Fe-MIL-101 was highly active in catalyzing the oxidation of TMB substrate by H_2O_2 . Moreover, the peroxidase-like activity of Fe-MIL-101 was confirmed by catalytic oxidation of other peroxidase substrates such as ABTS (2, 2'-azino-bis(3-ethylbenzothiazoline-6-sulfonic acid) diammonium salt). In the presence of H_2O_2 , these reactions could also produce a green color product (Fig. S5).

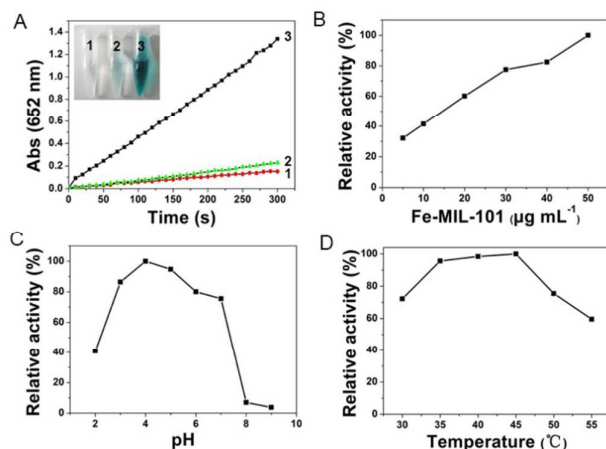


Fig. 1 (A) Time-dependent absorbance changes at 652 nm in the presence of TMB (1), H_2O_2 and TMB (2), H_2O_2 , TMB and Fe-MIL-101(3). [TMB]: 0.4 mM, [H_2O_2]: 5mM, [Fe-MIL-101]: 6.7 $\mu\text{g mL}^{-1}$. Inset shows corresponding photographs. (B, C, D) The peroxidase-like activity of the Fe-MIL-101 hybrid is dependent on catalyst amount (B), pH (C) and temperature (D). Experiments were carried out in acetate buffer (20 mM, pH 4.0).

The peroxidase-like catalytic activity of Fe-MIL-101 was investigated by selecting the substrates TMB and H_2O_2 as a model reaction system. The peroxidase-like activity of Fe-MIL-101 was measured while varying the catalyst concentration from 10 to 50 $\mu\text{g mL}^{-1}$, the pH from 2.0 to 9.0, the temperature from 30 °C to 55 °C (Fig. 1B-D), the H_2O_2 concentration from 0.01 mM to 0.8 mM and the TMB concentration from 0.05 mM to 0.5 mM (Fig. S6, S7). Fig. 1B showed the absorbance changes (at 652 nm) against different concentrations of Fe-MIL-101. Dramatic improvement of catalytic activity could be observed with the steady increase of Fe-MIL-101 concentration. Furthermore, like other nanomaterial-based peroxidase mimics, the activity of Fe-MIL-101 was also dependent on pH and temperature (Fig. 1C and 1D). Most notably, Fe-MIL-101 exhibited high activity over a broad pH range. As shown in Fig. 1C, the peroxidase-like activity of Fe-MIL-101 remained about 80 % at pH 7.0 compared to that at

pH 4.0. The optimal pH and temperature were pH 4.0 and 45 °C, which are very similar to the values for HRP.³⁵

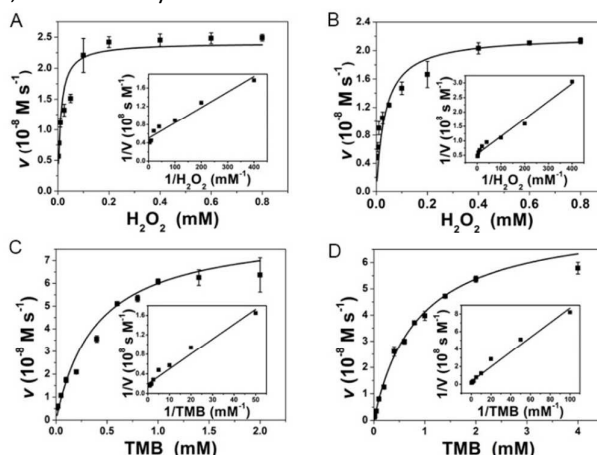


Fig. 2 Steady-state kinetic assays of the Fe-MIL-101. (A, C) The concentration of TMB was 0.2 mM and the H_2O_2 concentration was varied in acetate buffer at pH 4.0 (A) and borate buffer at pH 7.0 (C); inset: double-reciprocal plots of activity of Fe-MIL-101. (B, D) The concentration of H_2O_2 was 0.2 mM and the TMB concentration was varied in acetate buffer at pH 4.0 (B) and borate buffer at pH 7.0 (D); inset: double-reciprocal plots of activity of Fe-MIL-101. Error bars shown represent the standard error derived from three repeated measurements.

The peroxidase-like catalytic mechanism and kinetic parameters of Fe-MIL-101 were further investigated using steady-state kinetics. The kinetic data was obtained by varying one substrate concentration while keeping the other substrate concentration constant. Within the range of used TMB and H_2O_2 concentrations, typical Michaelis-Menten curves were observed (Fig. 2). A Lineweaver-Burk plot can be obtained with a nearly linear relationship (inset of Fig. 2) from which important kinetic parameters can be obtained (Table 1 and Table 2). The kinetic parameters, such as the Michaelis-Menten constant (K_m) and maximum initial velocity (V_{max}) were obtained from a Lineweaver-Burk plot. The Michaelis constant, K_m is a characteristic value irrelevant to the concentrations of substrate and enzyme, and is often associated with the affinity of the catalyst molecules for the substrate.²⁴ The greater the K_m value is, the weaker the binding between the enzyme and substrate. As shown in Table 1, the K_m value of Fe-MIL-101 with H_2O_2 as the substrate under the optimum conditions (20 mM acetate buffer, pH 4.0) was about 616-fold lower than HRP (3.7 mM) suggesting that Fe-MIL-101 has an extremely higher affinity for H_2O_2 than HRP. This value is about 6 times less than that of MIL-53 (Fe) ($K_m = 0.04$ mM) and about 1800 times less than that of H@M (Hemin@MIL-101 (Al)-NH₂) ($K_m = 10.9$ mM), respectively. Moreover, the K_m value of Fe-MIL-101 is also about 2-23000 fold less than other nanomaterials in supplementary Table S1. Thus, the value of K_m (0.006 mM) for Fe-MIL-101 is the lowest value of K_m reported so far to the best of our knowledge and it

has a higher affinity to H₂O₂ than all reported nanomaterials at pH 4.0.

In the following, the peroxidase-like activity of Fe-MIL-101 was evaluated at neutral pH (20 mM borate buffer, pH 7.0). Typical Michaelis-Menten curves (Fig. 2B and 2C) were received in a certain range of H₂O₂ or TMB concentrations. The Michaelis constant K_m was shown in Table 2. The apparent K_m value of Fe-MIL-101 with TMB as the substrate was approximate to the value of HRP and the artificial enzyme mimic (GO-AuNCs). Surprisingly, one feature of Fe-MIL-101 as the enzyme mimic was that the K_m value (0.01mM) with H₂O₂ as the substrate was even lower than that of the natural enzyme HRP (0.2 mM), indicating that Fe-MIL-101 had a higher binding affinity to H₂O₂. Meanwhile, the K_m value was also about 14000 fold less than that of reported GO-AuNCs at pH 7.0. The value of K_m (0.01mM) for Fe-MIL-101 is the lowest value of K_m reported so far to the best of our knowledge and it

has a higher affinity to H₂O₂ than all reported nanomaterials at pH 7.0. Another notable feature of the Fe-MIL-101 artificial enzyme was its high affinity to H₂O₂ over a broad pH range, especially at neutral pH. Fe-MIL-101 showed a surprisingly low K_m value of 0.01mM at neutral pH, which was only slightly higher than that of Fe-MIL-101 at acid pH (0.006 mM). On the basis of this unique and attractive property, Fe-MIL-101 will be applied into biological systems where a near neutral pH is required.

Michaelis-Menten curves are shown in Fig. S8 and the Michaelis-Menten constant (K_m) and maximum initial velocity (V_{max}) are summarized in Table 1 and Table 2. It is seen that the values of K_m for Fe-MIL-101-FA were slightly higher than that of Fe-MIL-101 (Table 1 and Table 2) but lower than that of most nanomaterials. Thus, Fe-MIL-101-FA preserved good peroxidase-like activity of Fe-MIL-101.

Table 1 Comparison of the kinetic parameters of different nanomaterials that mimic peroxidase at pH 4.0.

Catalysts	Substrates	K_m (mM)	V_{max} (M s ⁻¹)	Ref.
HRP	TMB	0.434	10.0×10 ⁻⁸	35
HRP	H ₂ O ₂	3.7	8.71×10 ⁻⁸	35
Fe ₃ O ₄ MNPs	TMB	0.098	3.44 ×10 ⁻⁸	35
Fe ₃ O ₄ MNPs	H ₂ O ₂	154	9.78×10 ⁻⁸	35
Fe ₃ O ₄ @C	TMB	0.313	1.98×10 ⁻⁷	36
Fe ₃ O ₄ @C	H ₂ O ₂	0.014	5.25×10 ⁻⁸	36
PCN-222 (Fe)	TMB	1.63	/	24
MIL-53 (Fe)	TMB	1.08	8.78×10 ⁻⁸	25
MIL-53 (Fe)	H ₂ O ₂	0.04	1.86×10 ⁻⁸	25
Fe-MIL-88NH ₂	TMB	0.284	1.047×10 ⁻⁷	27
Fe-MIL-88NH ₂	H ₂ O ₂	2.06	7.04×10 ⁻⁸	27
H@M	TMB	0.068	6.07×10 ⁻⁸	37
H@M	H ₂ O ₂	10.9	8.98×10 ⁻⁸	37
SDS-MoS ₂ NPs	TMB	2.04	1.6×10 ⁻⁸	38
SDS-MoS ₂ NPs	H ₂ O ₂	0.013	1.93×10 ⁻⁹	38
Fe-MIL-101	TMB	0.158	5.12×10 ⁻⁸	This work
Fe-MIL-101	H ₂ O ₂	0.006	1.98×10 ⁻⁸	This work
Fe-MIL-101-FA	TMB	0.164	1.31×10 ⁻⁸	This work
Fe-MIL-101-FA	H ₂ O ₂	0.027	1.55×10 ⁻⁸	This work

Table 2 Comparison of the Michaelis constant (K_m) of the Fe-MIL-101 and other enzyme at pH 7.0.

Catalysts	Substrates	K_m (mM)	Ref.
HRP	TMB	0.20	10
HRP	H ₂ O ₂	0.16	10
GO-AuNCs	TMB	0.16	10
GO-AuNCs	H ₂ O ₂	142.39	10
Fe-MIL-101	TMB	0.25	This work
Fe-MIL-101	H ₂ O ₂	0.01	This work
Fe-MIL-101-FA	TMB	0.39	This work
Fe-MIL-101-FA	H ₂ O ₂	0.02	This work

Mechanism of Peroxidase-Like Activity of Fe-MIL-101.

As previous work demonstrated Fe³⁺ ions are Fenton-like reagents, they could also catalyze TMB oxidation in the

presence of H₂O₂.^{39,40} In order to ensure the peroxidase-like activity is due to Fe-MIL-101 but not any component that leaches out from Fe-MIL-101 to the reaction solution, Fe-MIL-101 was centrifuged out at the end of the reaction and the

reaction mixture was analyzed by ICP. The concentration of iron ions in the supernatant of Fe-MIL-101 solution was not detected. Therefore, the observed reaction cannot be attributed to leaching of iron ions into solution, but occurs on the surface of Fe-MIL-101. The XRD pattern of the used Fe-MIL-101 was almost the same as the fresh one, indicating that Fe-MIL-101 was stable during the peroxidase reaction (Fig. S1). SEM images also show that the fresh and used Fe-MIL-101 are similar, again implying that Fe-MIL-101 was stable during the catalytic reaction. All these observations indicate that Fe-MIL-101 possesses peroxidase-like activity for oxidation of TMB in the presence of H_2O_2 .

The catalytic mechanism of Fe-MIL-101 was further investigated by the detection of hydroxyl radicals ($\bullet\text{OH}$) with a photoluminescence method, where terephthalic acid easily reacted with $\bullet\text{OH}$ to form highly fluorescent 2-hydroxy terephthalic acid.⁴¹ Fig. 3 shows that gradual increase of the fluorescence intensity was observed with the concentration of Fe-MIL-101 increased, suggesting that the amount of generated $\bullet\text{OH}$ was increased by Fe-MIL-101. However, there was no fluorescence intensity in the absence of Fe-MIL-101. These results indicated that Fe-MIL-101 could decompose H_2O_2 to generate the $\bullet\text{OH}$ radical. For the above reasons, a probable mechanism for peroxidase-like activity of Fe-MIL-101 has been proposed as following: H_2O_2 molecules were activated by Fe-MIL-101 to generate the $\bullet\text{OH}$, then TMB was oxidized by $\bullet\text{OH}$ to form an oxidized TMB which was shown blue color.

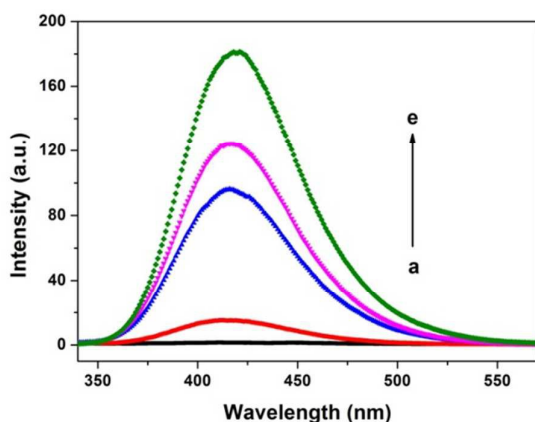


Fig. 3 The effect of Fe-MIL-101 on the formation of hydroxyl radical with terephthalic acid as a fluorescence probe. (a) $10 \mu\text{g mL}^{-1}$ Fe-MIL-101, without H_2O_2 , (b–e) 0, 10, 20, and $30 \mu\text{g mL}^{-1}$ Fe-MIL-101, $50 \text{ mM H}_2\text{O}_2$. Reaction conditions: 0.2 mM terephthalic acid and different solutions were incubated in acetate buffer ($\text{pH } 4.0$) at $40 \text{ }^\circ\text{C}$ for 30 min.

This mechanism was similar to that of natural enzymes in which the extraordinarily high catalytic efficiency was largely due to the ability to bring substrates into proximity with their active sites.¹⁰ In particular, the space confinement effect of

micropores in MOFs to biomacromolecules mimics the cage-like nature of active site in an enzyme.³⁰ Other characteristics of MOFs such as large specific surface area, stable well-defined crystalline open structure and great numbers of active sites,²⁴ can also benefit the efficiency. For example, BET surface area ($3700 \text{ m}^2 \text{ g}^{-1}$) of Fe-MIL-101 is much bigger than that of PCN-222(Fe)²⁴ ($2200 \text{ m}^2 \text{ g}^{-1}$). Moreover, it has been reported previously that peroxidase-like activity of Fe-based MOFs could originate from its catalytic activation of H_2O_2 through electron transfer to produce $\bullet\text{OH}$ radicals by a Fenton-like reaction^{25, 27-29}. Therefore, the uniqueness of Fe-MIL-101 may be relevant to its excellent ability to produce $\bullet\text{OH}$ radicals. When compared with other MOFs, especially MIL-53 (Fe), which possesses the highest affinity among the reported MOF materials, Fe-MIL-101 produced stronger fluorescence by using terephthalic acid as a probe.²⁵ This implied that the activity for producing $\bullet\text{OH}$ by decomposing H_2O_2 over Fe-MIL-101 was higher than MIL-53 (Fe). However, the detailed reasons and certain mechanism for the significant peroxidase-like activity of Fe-MIL-101 are not clear yet, deserve further investigation.

Cytotoxicity and cellular uptake of Fe-MIL-101-FA.

In order to examine the cells viability by MTT assay, KB, HeLa, HT-29 and BABL-3T3 cells were incubated in the presence of $20 \mu\text{g mL}^{-1}$ Fe-MIL-101-FA (a), $0.2 \text{ mM H}_2\text{O}_2$ (b), 0.2 mM TMB (c), $\text{H}_2\text{O}_2 + \text{TMB}$ (b + c) and Fe-MIL-101-FA + $\text{H}_2\text{O}_2 + \text{TMB}$ (a + b + c) for 12 hours. As shown in Fig. 4A, the four cells showed above 90% viability after cells treated with $20 \mu\text{g mL}^{-1}$ Fe-MIL-101-FA, suggesting Fe-MIL-101-FA has good biocompatibility and indicating the method of detection cancer was non-dependent on the viability of the cells. In addition, we detected the four cells viability under TMB, H_2O_2 , TMB + H_2O_2 , and TMB + H_2O_2 + Fe-MIL-101-FA conditions. It was observed that the viability of the cells was kept above 90% for 12 h under various conditions. Therefore, TMB (0.2 mM) and H_2O_2 (0.2 mM), TMB + H_2O_2 + Fe-MIL-101-FA did not do any significant harm to the cells.

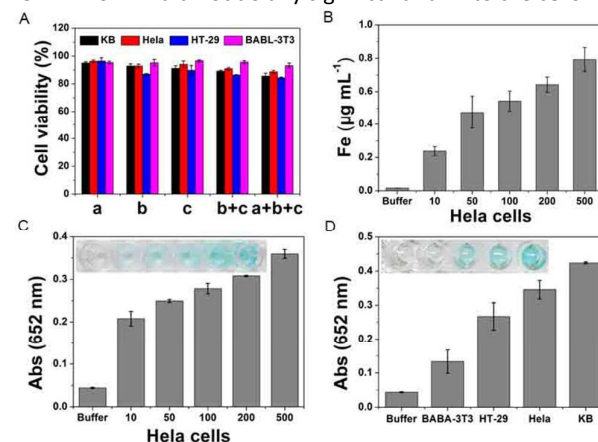


Fig. 4 (A) In vitro cell viability tests by MTT assay for KB, HeLa, HT-29 and BABL-3T3 cells in the presence of $20 \mu\text{g mL}^{-1}$ Fe-MIL-101-FA (a), $0.2 \text{ mM H}_2\text{O}_2$ (b), 0.2 mM TMB (c), $\text{H}_2\text{O}_2 + \text{TMB}$ (b+c) and Fe-MIL-101-FA + $\text{H}_2\text{O}_2 + \text{TMB}$ (a+b+c) for 12 hours. (B) The content of Fe^{3+} in HeLa cells measured by ICP-MS. (C) The absorption values at 652 nm after 400 s depend on the number of HeLa

cells. Inset: the color change with number of HeLa cells (from left to right: buffer, 10, 50, 100, 200 and 500 HeLa cells). (D) Fe-MIL-101-FA detection of folate receptor expressing cells (from left to right: Buffer, 500 BABL-3T3 cells, 500 HT-29 cells, 500 HeLa cells and 500 KB cells). Inset: typical photographs for cancer cell detection with the colorimetric method developed using Fe-MIL-101-FA. Data are expressed as mean \pm SD of three independent experiments.

Colorimetric detection for cancer cells by Fe-MIL-101-FA.

The peroxidase-like activity of Fe-MIL-101-FA was used to detect cancer cells. Different amounts of HeLa cells were first incubated with Fe-MIL-101-FA in DMEM medium for 1.5 hours. Then centrifuged and rinsed with PBS three times to remove the unattached Fe-MIL-101-FA. The ICP-MS analysis was used to study the cellular uptake efficacy of Fe-MIL-101-FA. As shown in Fig. 4B, as the number of HeLa cells increased, the content of Fe was increased, indicating that Fe-MIL-101-FA could conjugate with folate receptors effectively.

In the presence of TMB and H₂O₂, the Fe-MIL-101-FA conjugated cells would catalyze a color reaction, which can be distinguished by the naked eye and easily be quantitatively monitored by the absorbance at 652 nm. As the number of HeLa cells increased (10-500), the value of absorbance raised rapidly, suggesting that more Fe-MIL-101-FA bind to folate receptors on the surface of HeLa cells (Fig. 4C), which was consistent with the tendency of the content of Fe in cellular. As a result, we have found a relatively good linear correlation ($R^2 = 0.936$) between the number of HeLa cells and the absorbance in the range of 10 to 500 cells, and a better linear correlation ($R^2 = 0.987$) was obtained in the range of 50 to 500 cells (Fig. S9). Using this method, as low as 10 cells could be visualized clearly by naked eye, demonstrating good sensitivity of the method. The difference may be caused by many interference factors especially when the cell number was too little. Nevertheless, the detection limit is lower than the detection limit was lower than that reported in previously published studies involving cancer cell assays employing the peroxidase-like activity of most of nanomaterials, such as GO-FA-Hemin,⁵ FA-GO-AuNCs,¹⁰ and FA-CS-AgI¹² hybrids.

This colorimetric detection method also demonstrated the specificity of Fe-MIL-101-FA for cancer cells (Fig. 4D). Four cell lines (BABL-3T3, HT-29, HeLa and KB) were used in experiments. BABL-3T3 cells, as the normal cell line, did not overexpress folate receptors. As a contrast, HT-29, HeLa and KB cells were employed as cancer cell lines with overexpressed folate receptors.¹⁶ After culturing with cells for 1.5 h, Fe-MIL-101-FA showed much stronger binding to cancer cells (HT-29, HeLa and KB cells) than that of BABL-3T3 cells. The absorbance of Fe-MIL-101-FA with 500 target cells (HT-29, HeLa and KB) is significantly higher than the same amount of Fe-MIL-101-FA with 500 control cells (BABL-3T3), whereas the absorbance of KB cells was about 2.2 times higher than that of BABL-3T3 cells (Fig. 4D). These results indicate that the Fe-MIL-101-FA bound selectively to the target cells through the interaction between FA and folate receptor and that the assembly of Fe-MIL-101

around the target cells catalyzed the oxidation of TMB in the presence of H₂O₂. In addition, because of the different amounts of folate receptor expression on different types of cancer cells, more Fe-MIL-101-FA was bound to KB cells than HT-29 and HeLa cells. Since folate receptors were overexpressed on the cell membranes of different types of cancer cells, including ovarian, endometrial, colorectal, breast, lung, renal cell carcinomas, brain metastases derived from epithelial cancers, and neuroendocrine carcinomas, this method might be general for cancer cell detection,⁵ due to high-affinity and specificity to folate receptors.

In order to illustrate the interaction between Fe-MIL-101-FA and cancer cells, the zeta potentials of Fe-MIL-101 and Fe-MIL-101-FA were measured by Zetasizer Nano-ZS at pH 7.0 buffer. It is seen that zeta-potential value of Fe-MIL-101 (-22 ± 1.1) shifted to less negative values (-17.5 ± 0.7) after adsorption FA in PBS buffer. This is in accordance with previously reported data on FA-coated nanoparticles.⁴² In addition, the zeta potential was determined in DMEM cell culture media + 10% fetal bovine serum. Zeta-potential value of Fe-MIL-101 (-0.071 ± 0.01) shifted to positive value of Fe-MIL-101-FA (0.154 ± 0.03). This phenomenon was due to interaction between materials and the proteins in the medium.⁴³ However, the zeta potential value of HeLa cell membrane was about -8.4 ± 0.6 mV. There is a weak electrostatic adsorption between Fe-MIL-101-FA and cytomembrane of cancer cells. The major interaction may come from the conjunction of FA and folate receptors.

Since our MOF composite was synthesized simply by adsorption FA onto the surfaces of Fe-MIL-101, whereas above three mentioned composites usually requires amidation or sulfonation to conjugate FA. Moreover, compared to another expensive antibody functionalized- nanomaterials, such as HER2 antibody-conjugated GO_MNP-10-Pt-10 and DNA modified silver nanocluster ((DNA-Ag NCs), Fe-MIL-101-FA was lower-cost and more sensitive.

Conclusions

Fe-MIL-101 exhibited excellent peroxidase-like activity, catalyzing the oxidation of TMB and ABTS in the presence of H₂O₂ over broad pH range, even at neutral pH. The Michaelis constant (K_m) of Fe-MIL-101 with H₂O₂ as the substrate is about 616-fold (at pH 4.0) and 20-fold (at pH 7.0) smaller than free natural horseradish peroxidase (HRP), indicating a much higher affinity for H₂O₂ than HRP and most of the peroxidase mimetics. Moreover, Fe-MIL-101 was successfully used to detect cancer cells by conjugating folic acid onto Fe-MIL-101 without any surface modification. The detection limit of the method for HeLa was estimated to be as low as 50 cells and the reaction colour produced by 10 cells also could be observed by the naked eye. These findings mentioned above will open an avenue for using MOFs as enzymatic mimics in immunoassays and biotechnology.

Acknowledgements

The authors thank National Natural Science Foundation of China (Project 21573193) and Program for Innovation Team of Yunnan Province and Innovative Research Team (in Science and Technology) in Universities of Yunnan Province and Key Laboratory of Wastewater Treatment Materials of Kunming for financial support. The authors also thank Key project from Yunnan Educational Committee (Project ZD2012003) for financial support.

Notes and references

- I.H. El-Sayed, X. Huang, M.A. El-Sayed, *Nano Lett.*, 2005, **5(5)**, 829-834.
- W. Lu, S.R. Arumugam, D. Senapati, A.K. Singh, T. Arbnesi, S.A. Khan, H. Yu, P.C. Ray, *ACS Nano*, 2010, **4(3)**, 1739-1749.
- P. Paterlini-Brechot, N.L. Benali, *Cancer Lett.*, 2007, **253(2)**, 180-204.
- E. Song, J. Hu, C. Wen, Z. Tian, X. Yu, Z. Zhang, Y. Shi, D. Pang, *ACS Nano*, 2011, **5(2)**, 761-770.
- Y. Song, Y. Chen, L. Feng, J. Ren, X. Qu, *Chem. Commun.*, 2011, **47(15)**, 4436-4438.
- S. Ge, M. Sun, W. Liu, S. Li, X. Wang, C. Chu, M. Yan, J. Yu, *Sensor. Actuat. B-Chem.*, 2014, **192**, 317-326.
- L. Wu, J. Wang, J. Ren, W. Li, X. Qu, *Chem. Commun.*, 2013, **49(50)**, 5675-5677.
- Y. Dong, H. Zhang, Z.U. Rahman, L. Su, X. Chen, J. Hu, X. Chen, *Nanoscale*, 2012, **4(13)**, 3969-3976.
- L. Su, J. Feng, X. Zhou, C. Ren, H. Li, X. Chen, *Anal. Chem.*, 2012, **84(13)**, 5753-5758.
- Y. Tao, Y. Lin, Z. Huang, J. Ren, X. Qu, *Adv. Mater.*, 2013, **25(18)**, 2594-2599.
- L. Zhang, H. Deng, F. Lin, X. Xu, S. Weng, A. Liu, X. Lin, X. Xia, W. Chen, *Anal. Chem.*, 2014, **86(5)**, 2711-2718.
- G. Wang, X. Xu, L. Qiu, Y. Dong, Z. Li, C. Zhang, *ACS Appl. Mater. Inter.*, 2014, **6(9)**, 6434-6442.
- M.I. Kim, M.S. Kim, M. Woo, Y. Ye, K.S. Kang, J. Lee, H.G. Park, *Nanoscale*, 2014, **6(3)**, 1529-1536.
- S.K. Maji, A.K. Mandal, K.T. Nguyen, P. Borah, Y. Zhao, *ACS Appl. Mater. Inter.*, 2015, **7(18)**, 9807-9816.
- A. Asati, S. Santra, C. Kaittanis, S. Nath, J.M. Perez, *Angew. Chem. Int. Ed.*, 2009, **48(13)**, 2308-2312.
- N. Kohler, C. Sun, J. Wang, M. Zhang, *Langmuir*, 2005, **21(19)**, 8858-8864.
- P. Falcaro, A.J. Hill, K.M. Nairn, J. Jasieniak, J.I. Mardel, T.J. Bastow, S.C. Mayo, M. Gimona, D. Gomez, H.J. Whitfield, R. Riccò, A. Patelli, B. Marmiroli, H. Amenitsch, T. Colson, L. Villanova, D. Buso, *Nat. Commun.*, 2011, **2**, 237-330.
- Z. Gu, J. Park, A. Raiff, Z. Wei, H. Zhou, *ChemCatChem*, 2014, **6(1)**, 67-75.
- J. Lee, O. K. Farha, J. Roberts, K. A. Scheidt, S. T. Nguyen, J. T. Hupp, *Chem. Soc. Rev.*, 2009, **38**, 1450-1459.
- S. Ma, *Pure. Appl. Chem.*, 2009, **81(12)**, 2235-2251.
- J.L.C. Rowsell, O.M. Yaghi, *J. Am. Chem. Soc.*, 2006, **128(4)**, 1304-1315.
- C. Sun, X. Wang, X. Zhang, C. Qin, P. Li, Z. Su, D. Zhu, G. Shan, K. Shao, H. Wu, J. Li, *Nat. Commun.*, 2013, **4**.
- J. Yu, Y. Cui, H. Xu, Y. Yang, Z. Wang, B. Chen, G. Qian, *Nat. Commun.*, 2013, **4**.
- D. Feng, Z. Gu, J. Li, H. Jiang, Z. Wei, H. Zhou, *Angew. Chem. Int. Ed.*, 2012, **51(41)**, 10307-10310.
- L. Ai, L. Li, C. Zhang, J. Fu, J. Jiang, *Chem-Eur. J.*, 2013, **19(45)**, 15105-15108.
- H. Tan, Q. Li, Z. Zhou, C. Ma, Y. Song, F. Xu, L. Wang, *Anal. Chim. Acta.*, 2015, **856**, 90-95.
- Y.L. Liu, X.J. Zhao, X.X. Yang, Y.F. Li, *Analyst*, 2013, **138(16)**, 4526-4531.
- Z. Jiang, Y. Liu, X. Hu, Y. Li, *Analytical Methods*, 2014, **6(15)**, 5647-5651.
- J. Zhang, H. Zhang, Z. Du, X. Wang, S. Yu, H. Jiang, *Chem. Commun.*, 2014, **50(9)**, 1092-1094.
- B. Li, D. Chen, J. Wang, Z. Yan, L. Jiang, D. Duan, J. He, Z. Luo, J. Zhang, F. Yuan, *Sci. Rep.*, 2014, **4**, 6759.
- F. Manea, F.B. Houillon, L. Pasquato, P. Scrimin, *Angew. Chem. Int. Ed.*, 2004, **43(45)**, 6165-6169.
- L. Pasquato, P. Pengo, P. Scrimin, *Supramol. Chem.*, 2005, **17(1-2)**, 163-171.
- I.Y. Skobelev, A.B. Sorokin, K.A. Kovalenko, V.P. Fedin, O.A. Kholdeeva, *J. Catal.*, 2013, **298**, 61-69.
- X. Zhang, S. Gong, Y. Zhang, T. Yang, C. Wang, N. Gu, *J. Mater. Chem.*, 2010, **20(24)**, 5110-5116.
- L. Gao, J. Zhuang, L. Nie, J. Zhang, Y. Zhang, N. Gu, T. Wang, J. Feng, D. Yang, S. Perrett, X. Yan, *Nat. Nanotechnol.*, 2007, **2(9)**, 577-583.
- Q. Li, Tang, G. Xiong, X. Cao, Y. Chen, L. Xu, F. Tan, H. Sensor. *Actuat. B-Chem.*, 2015, **215**, 86-92.
- F. Qin, S. Jia, F. Wang, S. Wu, J. Song, Y. Liu, *Catal. Sci. Technol.*, 2013, **3(10)**, 2761-2768.
- K. Zhao, W. Gu, S. Zheng, C. Zhang, Y. Xian, *Talanta*, 2015, **141**, 47-52.
- W. He, H. Jia, X. Li, Y. Lei, J. Li, H. Zhao, L. Mi, L. Zhang, Z. Zheng, *Nanoscale*, 2012, **4(11)**, 3501-3506.
- J. Zhang, S. Rana, R.S. Srivastava, R.D.K. Misra, *Acta. Biomater.*, 2008, **4(1)**, 40-48.
- K. Ishibashi, A. Fujishima, T. Watanabe, K. Hashimoto, *J. Photoch. Photobio. A*, 2000, **134(1-2)**, 139-142.
- Z. Zhang, J. Jia, Y. Lai, Y. Ma, J. Weng, L. Sun, *Bioorg. Med. Chem.* 2010, **18**, 5528-5534.
- C. Tamames-Tabar, D. Cunha, E. Imbuluzqueta, F. Ragon, C. Serre, M.J. Blanco-Prieto, P. Horcajada, *J. Mater. Chem. B*, 2014, **2**, 262-271.

The table of contents

we take advantage of the folic acid conjugated Iron-based Metal-organic frameworks (Fe-MIL-101) without any surface modification to design and develop a simple, cheap, highly selective and sensitive colorimetric assay to detect cancer cells based on its intrinsic peroxidase-like activity over broad pH range.

